

NASA TECHNICAL
REPORT

NASA TR R-230



NASA TR R-230

e 1

100 COPY: F
00 00 00
00000000



USE OF FUSIBLE TEMPERATURE
INDICATORS FOR OBTAINING
QUANTITATIVE AERODYNAMIC
HEAT-TRANSFER DATA

by Robert A. Jones and James L. Hunt
Langley Research Center
Langley Station, Hampton, Va.



TECH LIBRARY KAFB, NM



0068513

USE OF FUSIBLE TEMPERATURE INDICATORS FOR OBTAINING
QUANTITATIVE AERODYNAMIC HEAT-TRANSFER DATA

By Robert A. Jones and James L. Hunt

Langley Research Center
Langley Station, Hampton, Va.

NATIONAL AERONAUTICS AND SPACE ADMINISTRATION

For sale by the Clearinghouse for Federal Scientific and Technical Information
Springfield, Virginia 22151 - Price \$2.00

USE OF FUSIBLE TEMPERATURE INDICATORS FOR OBTAINING
QUANTITATIVE AERODYNAMIC HEAT-TRANSFER DATA

By Robert A. Jones and James L. Hunt
Langley Research Center

SUMMARY

Some of the methods used for obtaining quantitative aerodynamic heat-transfer data by means of temperature-sensitive coatings are described and discussed. A method whereby data can be obtained on arbitrary shapes without the use of a reference body has been developed. In this method, the heat-transfer coefficients depend only upon the thermal properties of the model material and the time required for a visible phase change of a fusible temperature indicator which is applied to the model as a thin surface coating. The phase change is recorded by motion-picture photography, and charts are given which relate the time required for the phase change to occur to the heat-transfer coefficient. Data obtained by this method are compared with aerodynamic theory and with data obtained by the conventional thermocouple-calorimeter technique. Several configurations were tested in the Langley Mach 8 variable-density tunnel. The results indicate that this method can be very useful and that accurate data can be obtained.

INTRODUCTION

In 1958 a temperature-sensitive coating was used at the Langley Research Center for determining qualitative aerodynamic heating rates (ref. 1). Since that time a development program has been underway to perfect a technique whereby quantitative data could be obtained by this method. It was suggested in reference 1 that motion-picture photography could be used to map isotherms at successive times and that this information could be used to estimate the value of the heat-transfer rates. The coating utilized in reference 1 undergoes color changes at certain temperatures. These temperatures are known to be functions of exposure time or heating rate (refs. 1 and 2).

Several methods for obtaining quantitative data with this type of coating have been considered. One method is to measure the time required for the surface to reach the known temperature as indicated by a color change of the coating and to calculate the corresponding heat-transfer rate from the transient heat-conduction equation. Another method is to test a reference body made of the same material as the model (e.g., a sphere for which the heat-transfer rates could be easily calculated) either simultaneously with the model or at the same

test conditions and then to assume that areas on the model and sphere which underwent color changes at equal times had equal surface temperatures. If the depth of heat penetration is small compared with the model dimensions, then these areas would be expected to have equal heat-transfer rates. In reference 3 the reference sphere method was used with a color-change coating, and heat-transfer rates were determined for a rather complex shape.

The present authors have found several difficulties that are inherent in color-change coatings, which limit their usefulness in obtaining quantitative data. The primary cause for these difficulties appeared to be the dependence of the color-change temperature of the coating on ambient pressure. (The pressure dependent characteristics of one of these coatings and the difficulties which arise with use of it are given in appendix A.) The manufacturer's literature describes these color-change coatings as metallic salts, which at certain temperatures liberate water vapor, carbon dioxide, or ammonia and, in so doing, change color; therefore, it is not surprising that the color-change temperature varies with pressure. A few of these coatings have been found to change colors with no change in temperature over a range of pressures commonly encountered in hypersonic test facilities (ref. 4). In addition, at a given pressure, the color-change temperature appears to be somewhat dependent on the amount of moisture absorbed from the atmosphere. The colors themselves are not too distinct and the patterns obtained on a model are sometimes difficult to photograph. Also, the known variation of the color-change temperature with the heating rate or exposure time causes difficulties.

On the basis of these considerations, a search was made for a material that would undergo a visible change at a known temperature independent of heating rate or ambient pressure. A readily available commercial product seemed to meet these requirements. These materials undergo a visible phase change from an opaque solid to a clear liquid at known temperatures. Materials available have phase-change temperatures that range from 100°F to 2500°F (310.9°K to 1644.3°K) in increments as small as 3°F (1.67°K). (See ref. 5.) A method has been developed for obtaining quantitative heat-transfer rates on arbitrary shapes for which these materials are used to indicate surface temperature. In this method, the heat-transfer rates depend upon the time required for the phase change to occur and upon the thermal properties of the model wall. The time required for the phase change to occur is determined from motion-picture photography, and the heat-transfer coefficients are obtained from solutions of the transient one-dimensional heat-conduction equation for a semi-infinite slab. A brief description of this method is given in reference 4.

The purpose of this report is to give a detailed description of the method herein called the phase-change-coating method. The phase-change coatings are described and calibrations of the phase-change temperatures are given for a range of heating rates and ambient pressures. The apparatus, test technique, and model construction are discussed. An analytical solution of the transient heat-conduction equation is given along with charts of the aerodynamic heat-transfer coefficient as a function of time required for the phase change, model thermal properties, and test conditions. The accuracy of the present method is discussed and charts are given with the error in indicated heat-transfer coefficient for various possible errors in thermal properties, time, and phase-change temperature. Data obtained by this method for several configurations in

a hypersonic facility are presented and are compared with both theoretical data and data obtained by the conventional thin-skin thermocouple-calorimeter method.

SYMBOLS

The units used for the physical quantities defined in this report are given both in the U.S. Customary Units and in the International System of Units (SI). (See ref. 6.) Factors relating the two systems are given in appendix B.

c_p	specific heat at constant pressure
erfc	complementary error function, $\frac{2}{\sqrt{\pi}} \int_{\beta}^{\infty} e^{-\lambda^2} d\lambda$
h	aerodynamic heat-transfer coefficient
h_c	aerodynamic heat-transfer coefficient based on constant-property solution
h_v	aerodynamic heat-transfer coefficient based on variable-property solution
k	thermal conductivity
L	length
l	thickness of model wall or allowable depth of heat penetration
M_{∞}	free-stream Mach number
r	radius of curvature of nose
$R_{\infty, D}$	free-stream Reynolds number based on model diameter
s	surface distance
t	time
t_d	thermal diffusion time
T	temperature
T_{aw}	adiabatic wall temperature
T_{cc}	color-change temperature
T_i	initial temperature of model

T_{pc} temperature of phase change

$$\bar{T} = \frac{T_{pc} - T_i}{T_{aw} - T_i}$$

x distance normal to model surface

α thermal diffusivity, $k/\rho c_p$

$$\beta = \frac{h\sqrt{\alpha t}}{k}$$

θ angular distance from stagnation point of sphere

ρ density

λ dummy variable of integration

PHASE-CHANGE COATINGS

The materials used for phase-change coatings are readily available commercial products described in reference 5. These materials undergo a phase change from an opaque solid to a clear liquid at known temperatures. The materials available have phase-change temperatures that differ as little as 3° F (1.67° K) and range from 100° F to 2500° F (310.9° K to 1644.3° K); each material has a specific temperature with a tolerance of ±1 percent. These materials are relatively inert and have extremely low vapor pressure in both the solid and liquid states. As supplied by the manufacturer they are suspended in an inert, volatile, nonflammable vehicle which can be mixed with a special thinner and sprayed on a model. When the model is sprayed with a very thin (less than 0.001 inch (2.54×10^{-3} cm)) coating of this material, it appears to be covered with small opaque crystals. When the coating melts, it becomes transparent and good contrast between the solid and liquid regions can be obtained by using a dark colored model. With care these coatings can be made sufficiently thin so that, for the present conditions, running of the melted coating and errors due to the latent heat of melting are negligible and yet the contrast is adequate for black-and-white photography. Tests made with a special calibration apparatus for coatings of different thickness indicated that the phase-change temperature was insensitive to the actual coating thickness provided the thickness was less than about 0.001 inch (0.254 cm). However, just enough phase-change material should be sprayed on the model to fog the surface (or just enough to be visible) in order to avoid running of the melted coating in wind-tunnel tests. The materials used in this investigation had phase-change temperatures of 125°, 150°, 175°, 200°, and 250° F (324.8°, 338.7°, 352.6°, 366.5°, and 394.3° K).

In order to ascertain the effects of heating rate and pressure on the phase-change temperature, a calibration apparatus was constructed which allowed

the measurement of phase-change temperature over a wide range of heating rates and ambient pressures. This apparatus consisted of a thin stainless-steel plate instrumented with thermocouples on the top surface and heated from below by a radiant heat source. The temperatures were recorded on magnetic tape by a high-speed analog-to-digital converter. Sample photographs of the phase-change patterns obtained with this calibration apparatus are shown in figure 1. The phase change is taking place at the line separating the light and dark areas. The melted coating or dark area was subjected to the higher heating rates.

Calibration tests were made for various heating rates in which the rate of change of surface temperature ranged from 1° F per second to 125° F per second (0.56° K/sec to 69.44° K/sec) at atmospheric pressure. The effect of pressures lower than 1 atmosphere ($101\ 325\ \text{N/m}^2$) was determined by placing the calibration apparatus in a bell jar and repeating the procedure for pressures as low as 3 millimeters of mercury absolute ($399.9\ \text{N/m}^2$). Sample results of these tests are presented in figure 2. For low heating rates the progression of the phase-change isotherm over the surface of the calibration plate was observed by eye. When the isotherm reached a thermocouple-plate juncture, a signal was placed on the magnetic tape by manually closing a limit switch and thereby identification was made of the temperature at which the phase change occurred. For the higher heating rates (above about 15° F per second (8.33° K/sec)) the progression of the isotherm over the calibration plate was photographed with a 35-mm time-study motion-picture camera. Synchronized electrical circuits for the camera and recorder provided a reference time for the two sets of data so that the temperature at a thermocouple location could be determined at the time the phase-change isotherm reached the thermocouple. The time, surface temperature, and rate of change of surface temperature with time for which the phase change occurred at each thermocouple were obtained from these records. All data shown in figure 2 are believed to be accurate to $\pm 4^{\circ}$ F

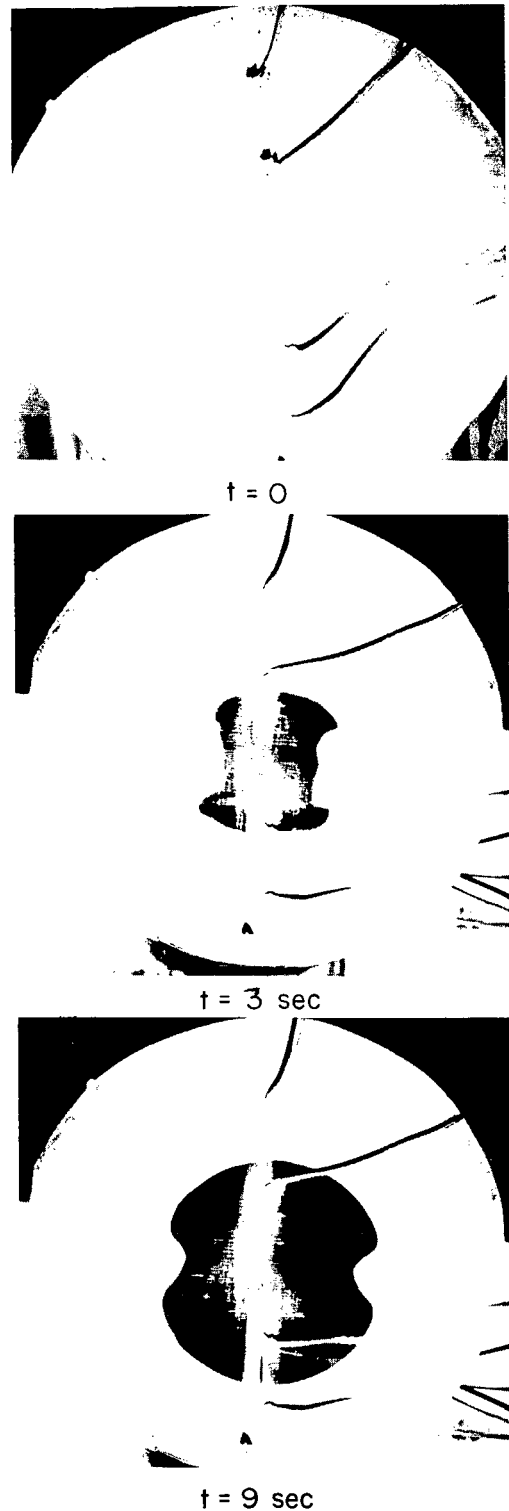


Figure 1.- Photographs of phase-change patterns in calibration apparatus.

L-65-7965

(2.22° K); however, at low heating rates the data are more accurate. These data were used only to determine the variation of phase-change temperature with heating rate and pressure rather than the actual value of the phase-change temperature. The effects of pressure and heating rate shown in figure 2 are considered to be negligible and the values quoted by the manufacturer for the phase-change temperature with an accuracy of ±1 percent appear to be correct within the range of these tests. Therefore the phase-change temperatures listed by the manufacturer were used for the data of this report.

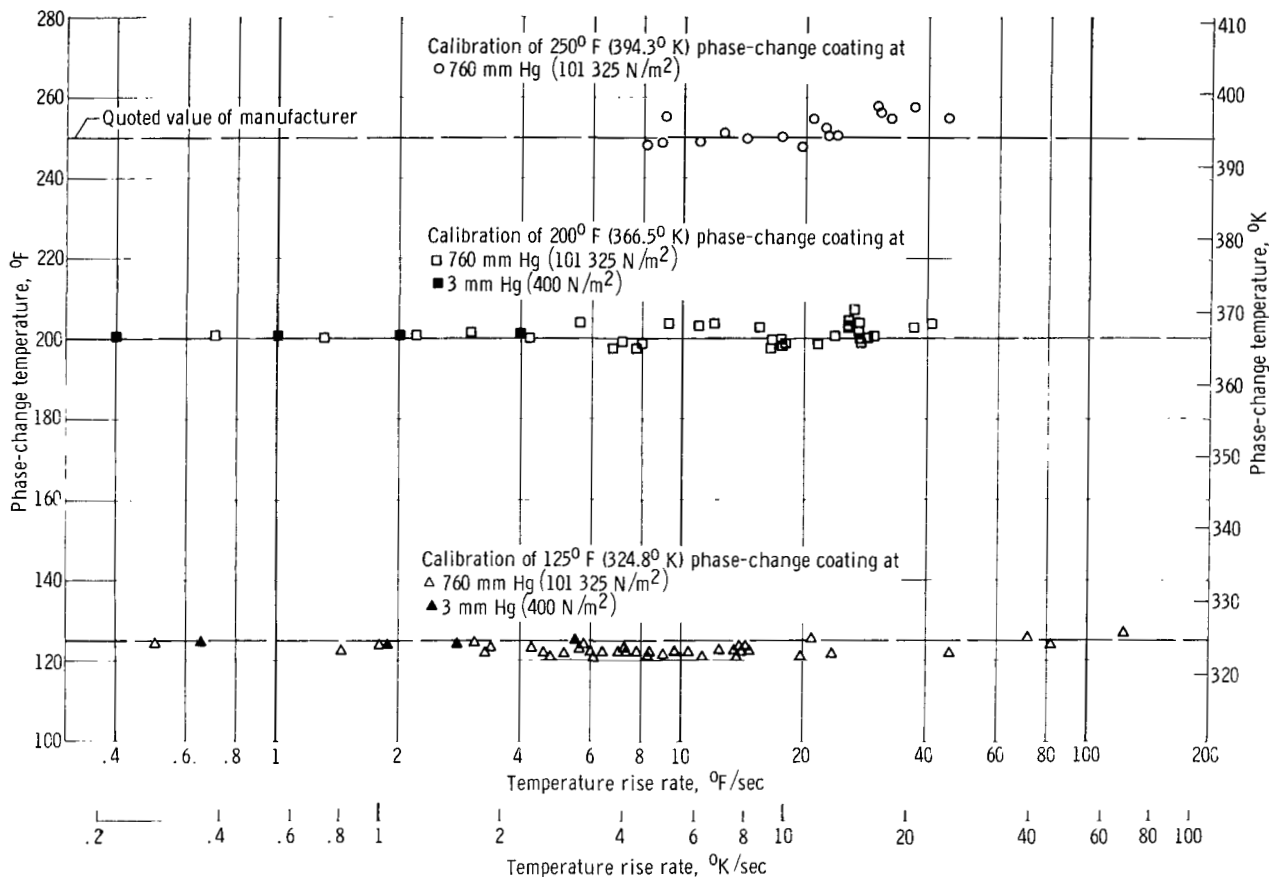


Figure 2.- Sample results of phase-change calibrations.

TEST TECHNIQUE AND PHOTOGRAPHY

The first step in the test procedure was to photograph a model on which a grid had been painted as a reference for determining surface locations. This stand-in model was placed in the exact position where the test model was to be placed. The test model was then sprayed with a phase-change material and mounted on the model injection mechanism which was in the retracted position so that during the tunnel starting period the model was not exposed to the airstream and thus remained isothermal. The tunnel was started and brought to the desired operating conditions. Then the camera and lights were started and the model was rapidly injected into the steady airstream. The injection time - that

is, the time from which the model first encounters the tunnel boundary layer until it is positioned in the uniform flow - was about 0.05 second. Between tests the model was taken out of the tunnel, the phase-change coating was washed off with thinner, the model was cooled until it was isothermal at room temperature, and then a new coating of phase-change material was sprayed on the model. Lines of constant heat-transfer coefficient were located by projecting the films of the phase-change patterns on enlarged photographs of the grid model.

The progression of the phase-change patterns over the model was recorded on high-speed 35-mm black-and-white film by using a special time-study data camera and stroboscopic xenon flash lamps. This camera is driven by a synchronous motor through interchangeable gears which allow exact framing rates of either 10, 20, or 30 frames per second. It is also equipped with two reference timing lights which can be used to put marks on the film margin for time correlation. The film is exposed in a double-frame format which gives negatives of about 24 mm by 36 mm. The model was lighted and photographed through windows in the tunnel test section. A photograph of a typical test setup is presented as figure 3.

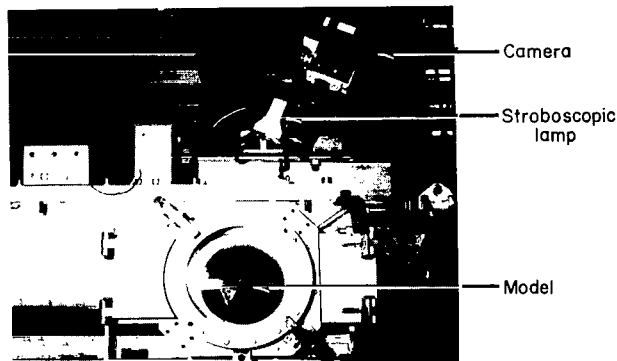


Figure 3.- Typical test setup. L-64-8370.1

THEORY FOR HEAT-TRANSFER COEFFICIENT

Semi-Infinite Slab Solution

In the method described herein the heat-transfer coefficients depend on the time required for the phase change to occur, the test conditions, and the thermal properties of the model wall. The relationship between the heat-transfer coefficient and the other parameters is determined from the solution to the equation governing the transient one-dimensional flow of heat. This equation is

$$\frac{\partial T}{\partial t} = \alpha \frac{\partial^2 T}{\partial x^2} \quad (1)$$

with the following initial and boundary conditions which most nearly describe the actual tunnel transient test:

$$T(x,0) = T_i \quad (2)$$

$$T(\infty, t) = T_i \quad (3)$$

$$\frac{\partial T(0, t)}{\partial x} = \frac{h}{k} [T_{aw} - T(0, t)] \quad (4)$$

It is assumed that the phase-change coating is at the surface temperature $T(0, t)$ and the time t is required when $T(0, t) = T_{pc}$ (T_{pc} is the temperature at which the phase change occurs). Other assumptions are as follows:

(1) The depth of heat penetration into the wall is small compared with the wall thickness and surface radius of curvature so that the wall acts like a semi-infinite slab (eqs. (1) and (3)).

(2) The model is isothermal before injection into the airstream (eq. (2)).

(3) The surface experienced an instantaneous step in aerodynamic heat-transfer coefficient at time zero and this coefficient is invariant with time (eq. (4)); this condition is normally encountered in a wind tunnel with constant stagnation conditions for a laminar boundary layer and rapid injection of the model.

(4) The thermal diffusivity α of the wall is invariant with temperature.

The solution of equation (1) is given in reference 7. With the specified boundary conditions, equation (1) can be written here in terms of parameters of interest as

$$\bar{T} = 1 - e^{\beta^2} \operatorname{erfc} \beta \quad (5)$$

where

$$\bar{T} = \frac{T_{pc} - T_i}{T_{aw} - T_i} \quad (6)$$

$$\beta = \frac{h}{k} \sqrt{\alpha t} \quad (7)$$

$$\operatorname{erfc} = \frac{2}{\sqrt{\pi}} \int_{\beta}^{\infty} e^{-\lambda^2} d\lambda \quad (8)$$

Equation (5) is plotted in figure 4 in terms of the parameter β as a function of \bar{T} . The parameter β depends on the properties of the wall, the aerodynamic heat-transfer coefficient, and the time required for the phase change to occur.

For a given set of conditions and a known time for the phase change, the heat-transfer coefficient can be computed from equation (7). (A full-page copy of figure 4 is inserted at the end of this report for the working convenience of the reader.)

An alternate plot of equation (5) is given in figure 5. In this figure the parameter $\frac{h}{k}\sqrt{\alpha}$ is plotted as a function of time for various values of \bar{T} . If the model properties are known, the heat-transfer coefficient can be read directly from this plot; however, interpolation between the different values of \bar{T} is required.

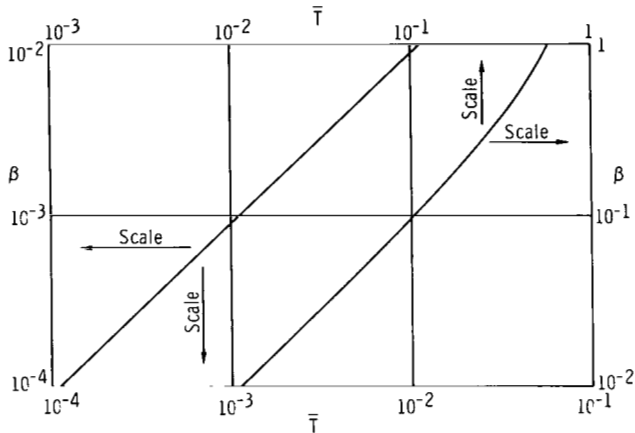


Figure 4.- Solution of heat-conduction equations (plot of eq. (5)).

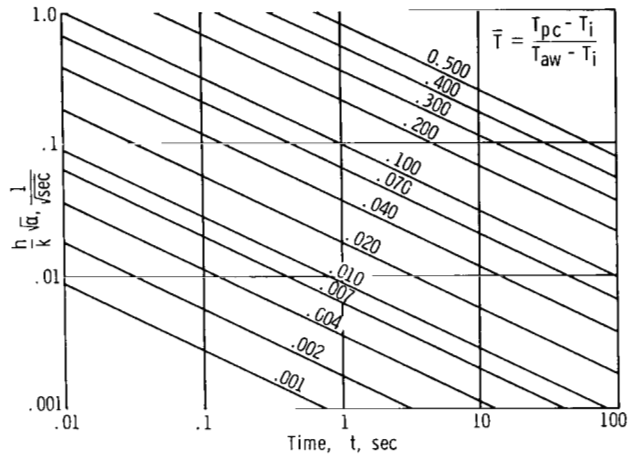


Figure 5.- Alternate plot for the solution of heat-conduction equations.

Thermal Diffusion Time

The time required for the phase change to occur should be large compared with the time from initial exposure of the model until steady flow is established in order to minimize errors due to the erroneous heating rates encountered while the model is passing through the tunnel boundary layer and errors due to the accuracy of determining the initial time. (These errors are discussed in a subsequent section of this report.) However, the time required for the phase change to occur must be short compared with the thermal diffusion time of the wall as this is one of the boundary conditions (eq. (3)). This thermal diffusion time t_d is independent of the aerodynamic heat-transfer coefficient and depends only on the thermal diffusivity of the wall and the allowable depth l of heat penetration. The thermal diffusion time is given approximately by the following equation:

$$\frac{\alpha t_d}{l^2} \approx 0.2 \quad (9)$$

Equation (9) was obtained by assuming a cubic distribution of temperature with depth in a slab subjected to an instantaneously applied constant heat-transfer rate at one surface and solving for the value of t_d for which a significant

change in temperature occurred at the depth l . In order to meet the necessary condition that the time required for the phase change to occur be short compared with the thermal diffusion time of the wall, the allowable depth of heat penetration l must be small compared with pertinent model dimensions, such as wall thickness, nose radius, corner radius, that is, for any given model dimensions the maximum allowable time for a phase change to occur is t_d . In practice, however, the time required for the phase change to occur can be controlled by selecting a coating material with a suitable value of T_{pc} . It may sometimes be desirable to spray different areas of a model with coating materials having different values of T_{pc} . To insure a reasonably long thermal diffusion time, the model wall should have a very low thermal conductivity which also should minimize any lateral conduction along the surface.

Comparison of Semi-Infinite Slab Solution With Finite Slab Solution

In order to check both the usefulness of the infinite-slab constant-property solution (eq. (5)) and the method given for determining the depth of heat penetration (eq. (9)), a computation was made for a finite slab 1/4 inch (0.635 cm) thick with thermal properties corresponding to those for one of the model walls used in this investigation. This computation was made by using the numerical analysis method of reference 8, an aerodynamic heat-transfer coefficient of 0.001 Btu/ft²-sec-°F (20.43 W/m²-°K), an initial temperature of 75° F (297.0° K), and an adiabatic wall temperature of 940° F (777.6° K). The slab material had the following thermophysical properties:

$$\rho = 117.6 \text{ lb/ft}^3 \quad (1883.95 \text{ kg/m}^3)$$

$$c_p = 0.2163 \text{ Btu/lb-}^\circ\text{F} \quad (905 \text{ J/kg-}^\circ\text{K})$$

$$k = 0.79 \times 10^{-4} \text{ Btu/ft-sec-}^\circ\text{F} \quad (4.919 \times 10^{-1} \text{ J/m-sec-}^\circ\text{K})$$

The resulting temperature-time variations of the front and back surfaces of the 1/4-inch-thick slab are shown in figure 6 in which the surface temperature of a semi-infinite slab having the same properties (eq. (5)) is also

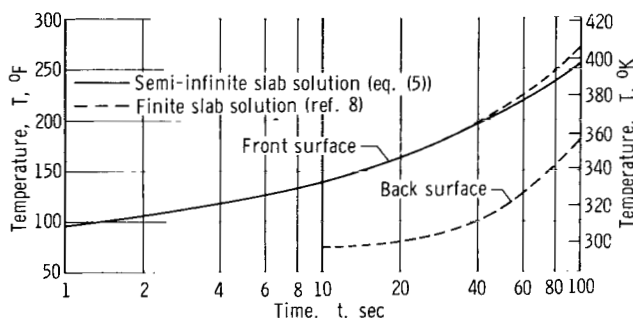


Figure 6.- Effect of finite slab on surface temperature.

included. Note that the front surface temperatures for the 1/4-inch-thick (0.635 cm) slab and semi-infinite slab are nearly the same for as long as 35 seconds. For the same conditions, material properties, and slab thickness, equation (9) gives a thermal diffusion time of 29 seconds. Therefore, equation (9) gives a conservative value for the thermal diffusion time or time for which the infinite slab solution (eq. (5)) is valid.

Effects of Temperature Dependent Properties
on Semi-Infinite Slab Solution

All models used in obtaining the phase-change-coating data presented in this report were constructed from a fiber-glass-reinforced plastic. The specific heat, thermal conductivity, and density of samples of this wall material were measured by a private corporation. (A description of the methods used in obtaining these values is given in ref. 9.) The quoted accuracy was ± 2 percent for specific heat at constant pressure, ± 3 percent for thermal conductivity, and ± 1 percent for density. The values of these properties for the fiber-glass-reinforced plastic at various temperatures are listed in the following table:

T		ρ		c_p		k	
$^{\circ}\text{F}$	$^{\circ}\text{K}$	lb/ft ³	kg/m ³	Btu/lb- $^{\circ}\text{F}$	J/kg- $^{\circ}\text{K}$	Btu/ft-sec- $^{\circ}\text{F}$	J/m-sec- $^{\circ}\text{K}$
75	297.0	119.1	1902.8	0.1987	831.4	0.77×10^{-4}	0.4794
100	310.9	118.7	1901.4	.2163	905.0	.79	.4919
125	324.8	118.3	1894.9	.2288	957.3	.78	.4857
150	338.7	117.8	1887.0	.2369	991.2	.80	.4981
175	352.6	117.4	1880.6	.2545	1064.8	.80	.4981
200	366.5	116.9	1872.6	.2994	1252.7	.83	.5168
225	380.4	116.5	1866.2	.2699	1129.3	.83	.5168
250	394.3	116.1	1859.7	.3055	1278.2	.84	.5230

The variation of these properties, particularly specific heat, with temperature is appreciable. In the solution of the heat-conduction equation the material properties appear as the parameter $\sqrt{\alpha}/k$ (eq. (7)). The data shown herein were reduced by using the average value of $\sqrt{\alpha}/k$ for the temperature range from 75 $^{\circ}$ F (297.0 $^{\circ}$ K) (approximate initial temperature) to the phase-change temperature T_{pc} . These values are as follows:

T_{pc}		$\frac{\sqrt{\alpha}}{k}$	
$^{\circ}\text{F}$	$^{\circ}\text{K}$	ft ² -sec ^{1/2} - $^{\circ}\text{F}/\text{Btu}$	m ² -sec ^{1/2} - $^{\circ}\text{K}/\text{J}$
125	324.8	22.6	1.11×10^{-3}
150	338.7	22.4	1.10
200	366.5	21.0	1.03

In order to evaluate the effects of the variation of material properties (c_p and k) with temperature, the numerical analysis method of reference 8 was used to obtain heat-transfer coefficients for the actual variable properties listed previously by interpolating linearly between the eight temperatures for which the properties were measured. In figure 7, the heat-transfer coefficients determined by this method for variable properties are compared with values

obtained by use of equation (5). The data are shown as the ratio of the heat-transfer coefficient h_v determined from the variable-property finite-slab solution of reference 8 to the heat-transfer coefficient h_c determined from the constant-property infinite-slab solution of equation (5) as a function of time for several values of phase-change temperature and various heat-transfer coefficients ranging from 0.001 to 0.01 Btu/ft²-sec-°F (20.43 to 204.3 W/m²-°K). It is thought that the effects of the variation in thermophysical properties with temperature indicated in figure 7 are small enough to be considered negligible.

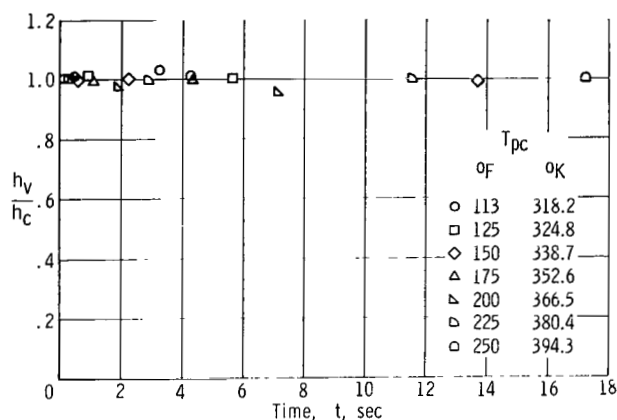


Figure 7.- Effect of variable thermal properties on heat-transfer coefficients.

ACCURACY

Several factors affecting the accuracy of this phase-change-coating method have already been considered in the previous section and are not repeated here. One factor that is considered is radiation. Since the model wall must be made from a good insulating material, care was taken to avoid errors due to radiation. The walls of the tunnel remained at nearly room temperature during a test and the temperatures at which the phase change occurred were relatively low so that radiation from these sources was negligible. However, it was found that radiation from photoflood lamps could introduce a considerable error. Photoflood lamps set at an intensity suitable for photography were found to melt the lower phase-change-temperature coatings in only a few seconds or on the same order of time as required for the lower aerodynamic heat-transfer rates. This problem was eliminated by the use of high-intensity electronic stroboscopic lamps which were synchronized with the camera shutter. Although these lamps had a high intensity, the duration of a single flash was only 25 microseconds so that the total on time of the lamps at the highest framing rate was only 0.75×10^{-3} second per second of test time or less than 0.1 percent.

Errors due to the accuracy with which the phase-change temperature is known, the accuracy with which the thermophysical properties of the wall are known, and the accuracy of determining the initial time ($t = 0$) all have an effect on the accuracy of the heat-transfer coefficient which can be evaluated by use of equations (5), (6), and (7). The maximum percent error in heat-transfer coefficient has been calculated by assuming errors of ± 3 percent in k , ± 2 percent in c_p , ± 1 percent in ρ , ± 1 percent in T_{pc} , and 0.1 second in time and is shown in figure 8 as a function of time for three different phase-change coatings. The percent errors used for these factors are the maximum errors quoted by the company which performed the thermophysical property measurements, the maximum errors quoted by the manufacturer of the phase-change coating, and an error in initial time which was thought by the authors to be the maximum

error possible with the technique used herein. The maximum percent error in heat-transfer coefficient (shown in fig. 8) is independent of the magnitude of the heat-transfer coefficient. In addition, the time variation of this error is due only to the error in initial time. The errors introduced by errors in thermophysical properties and phase-change temperature are invariant with time. Two sources of error which have not been considered in figure 8 but which appear in the value of \bar{T} used (eq. (6)) are T_{aw} and T_i . For the experimental results given in this report T_{aw} was calculated by using the appropriate entropy, the estimated local pressure, and a laminar recovery factor. The adiabatic wall temperature is always near the total temperature, and for most hypersonic facilities the difference $T_{aw} - T_i$ is very large compared with any possible error in T_{aw} so that T_{aw} can be neglected as a source of error.

The accuracy of T_i depends on the device used to measure it and generally initial temperature can be determined accurately. However, the difference $T_{pc} - T_i$ is not always large so that the error in \bar{T} due to the error in T_{pc} becomes larger for coatings having smaller values of T_{pc} . It is essential, therefore, to cool the model to near room temperature for each test, particularly for low values of T_{pc} .

For these tests, the initial time ($t = 0$) was taken to be that of the first frame of film which showed the model in the tunnel free stream. Inasmuch as the model actually encountered the airflow a short time before this so-called initial time, there is an error in the initial time due to the elapsed time from the instant the model first encounters the separated tunnel boundary layer until it is positioned in the free stream. This time was about 0.05 second for these tests. There is also an error in initial time due to the finite framing rate of the camera. The initial time can only be determined to the nearest frame; therefore, since the framing rate was 20 per second for most of these tests, the maximum of this error was 0.05 second. The maximum error in initial time is the sum of these two errors or 0.10 second for these tests; however, a more realistic estimate of the error could be made.

Since the error in initial time Δt is one error over which the experimentalist has some control, it has been considered in more detail in figure 9. As the time required for the phase change to occur becomes very large, the error due to an error in initial time approaches zero; however, this error is large at short times. Two things can be done to reduce the error in h due to an error in initial time Δt . First, the model should be injected into the airstream as rapidly as possible with the camera running at a fairly high framing rate to reduce the error in initial time Δt . Rapid injection also reduces the effects of the erroneous heating rates encountered while the model is passing through the tunnel boundary layer. Second, the value of the phase-change temperature T_{pc} should be selected to obtain reasonably long times; however, the time must not exceed the thermal diffusion time.

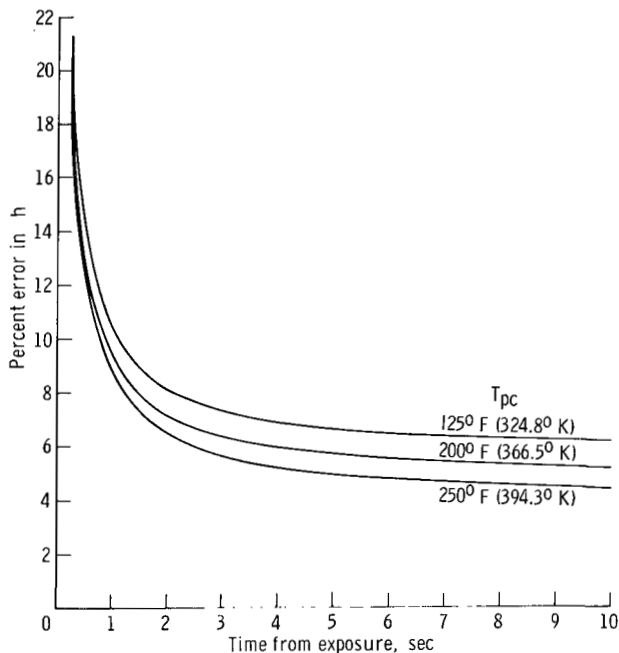


Figure 8.- Maximum percent error in h for three phase-change coatings. $T_{aw} = 900^{\circ}F$; $T_i = 75^{\circ}F$.

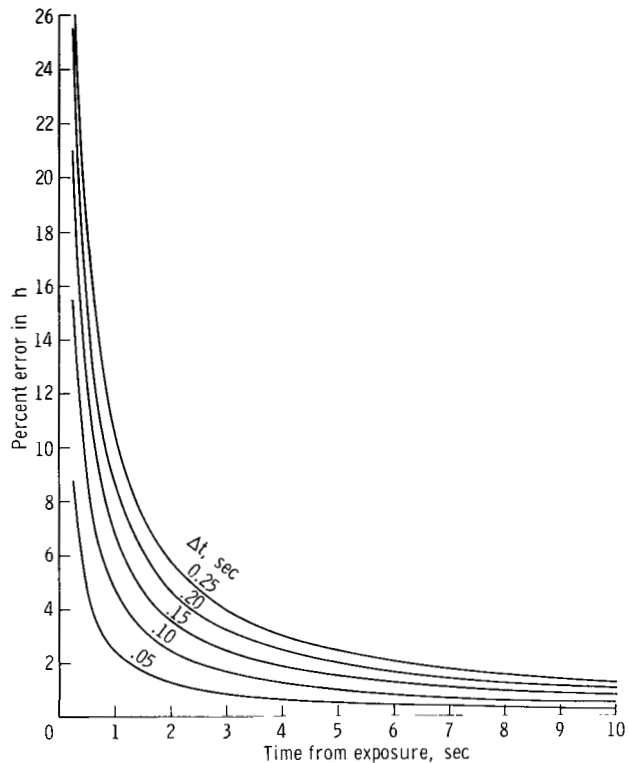


Figure 9.- Error in heat-transfer coefficient h due to an error in initial time Δt .

MODEL CONSTRUCTION

The conditions that should be considered in designing a model for use with this phase-change method are as follows:

(1) The thermal diffusivity of the material should be small enough to insure accuracy with the one-dimensional semi-infinite slab solution and to keep lateral conduction to a minimum, and yet sufficient to give adequate test time although the test time can be controlled by the T_{pc} used.

(2) The model must withstand high injection accelerations.

(3) The model must withstand thermal shock and relatively high temperatures depending upon the enthalpy of the facility, heating rate, and exposure time.

(4) The model wall material must be uniform to insure accurate determination of its thermophysical properties and should be such that the properties will be repeatable in making more than one model.

(5) The model surface must be impervious to the test fluid and to the paint and thinner used.

(6) The color of the model surface should be dark to provide sufficient contrast with the unmelted coating.

Experience gained with several different materials of which models have been made has indicated that the fiber-glass-reinforced plastic used in the present investigation is not the most desirable material primarily because of its nonuniformity. It was found that models made by different technicians or from different batches of material did not have the same thermophysical properties. A high-temperature epoxy plastic was found which had sufficient strength without fiber-glass reinforcement. This material is excellent for applications where the maximum surface temperature will not exceed 500° F (533.15° K). For testing in high-enthalpy facilities where some portion of the model surface is likely to reach a temperature in excess of 500° F (533.15° K), ceramics should be considered as a material. One glass-ceramic material investigated was suitable in all respects except for a porous white flat surface. It was found that a 1000-angstrom-thick coating of Cr₂O₃ could be placed on the surface by vapor deposition which would completely seal the surface, give it a dark color, and be thin enough to have negligible effect on the thermophysical properties. However, other ceramic materials are probably available which are nonporous and dark colored and are therefore more suitable for use at high enthalpies.

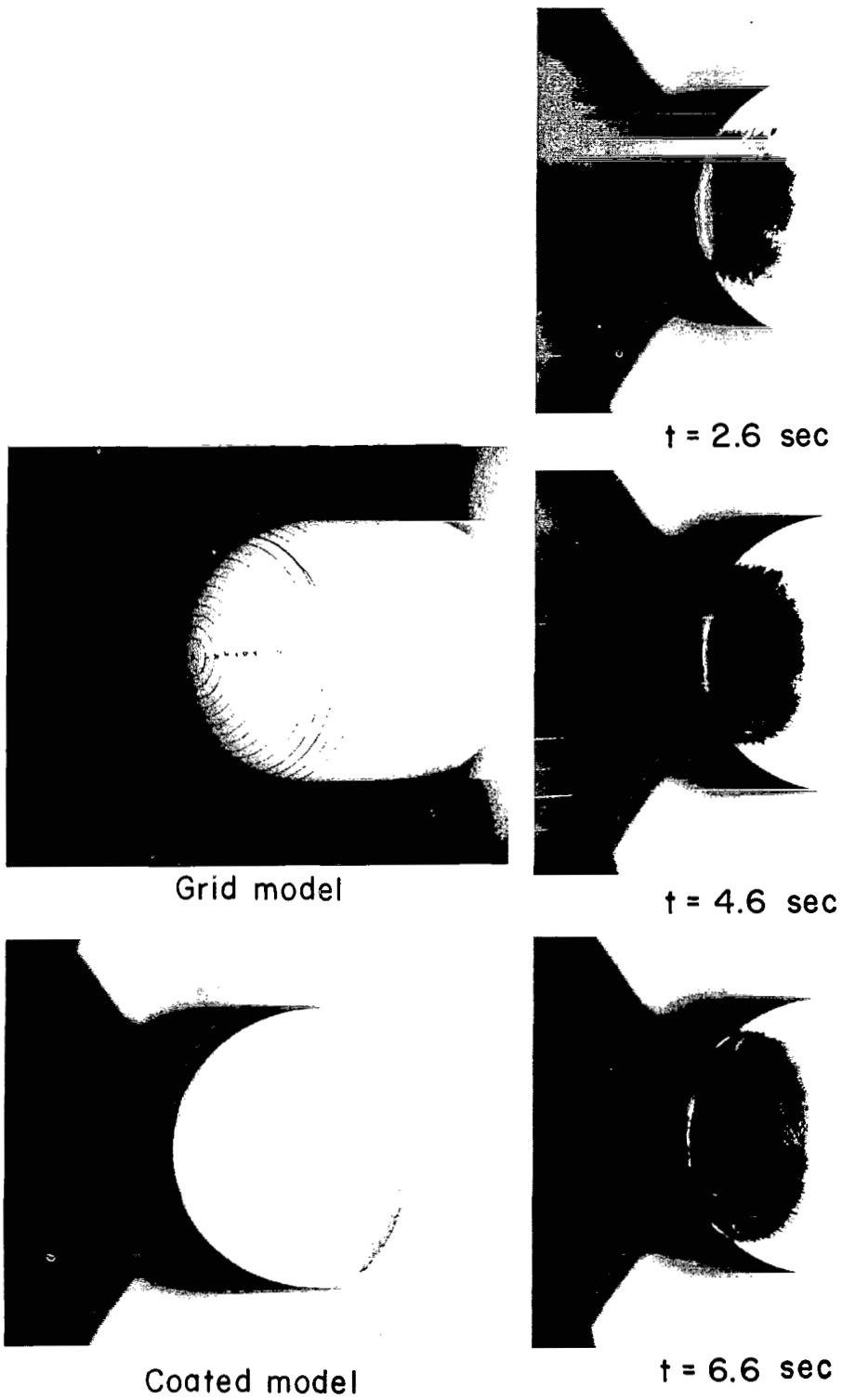
EXPERIMENTAL RESULTS AND DISCUSSION

Heat-transfer data have been obtained for several configurations at hypersonic speeds by use of the phase-change-coating method. All data presented herein were obtained in the Langley Mach 8 variable-density tunnel which has an axisymmetric contoured nozzle with an 18-inch-diameter (0.4572 m) test section and operates as a blowdown facility by exhausting to a 41-foot-diameter (12.497 m) vacuum sphere. Maximum tunnel operating times are approximately 2 minutes (120 sec); however, these tests required about 15 seconds. A description of the characteristics of this facility is given in reference 10.

Hemisphere-Cylinder

A 4-inch-diameter (10.16 cm) hemisphere-cylinder was tested at free-stream Reynolds numbers of 2×10^5 , 3.4×10^5 , and 6.8×10^5 based on model diameter and at zero angle of attack. This hemisphere-cylinder model was constructed by forming a layer of fiber-glass-reinforced plastic over an aluminum mandrel. Two thermocouples were attached at the plastic-aluminum interface to monitor the initial temperature. The 200° F (366.5° K) phase-change coating was used for each test. The grid model and coated model positioned in the test section prior to the test are shown in figure 10(a). Sample photographs of the phase-change patterns obtained during one of the tests are shown as figure 10(b).

The heat-transfer-coefficient distributions obtained for the three Reynolds numbers are compared with theoretical distributions in figure 11.



(a) Grid and coated models with no airflow.

(b) Phase-change patterns on coated model. $T_{pc} = 200^{\circ}$ F.

Figure 10.- Photographs of 4-inch-diameter hemisphere-cylinder models. L-65-7966

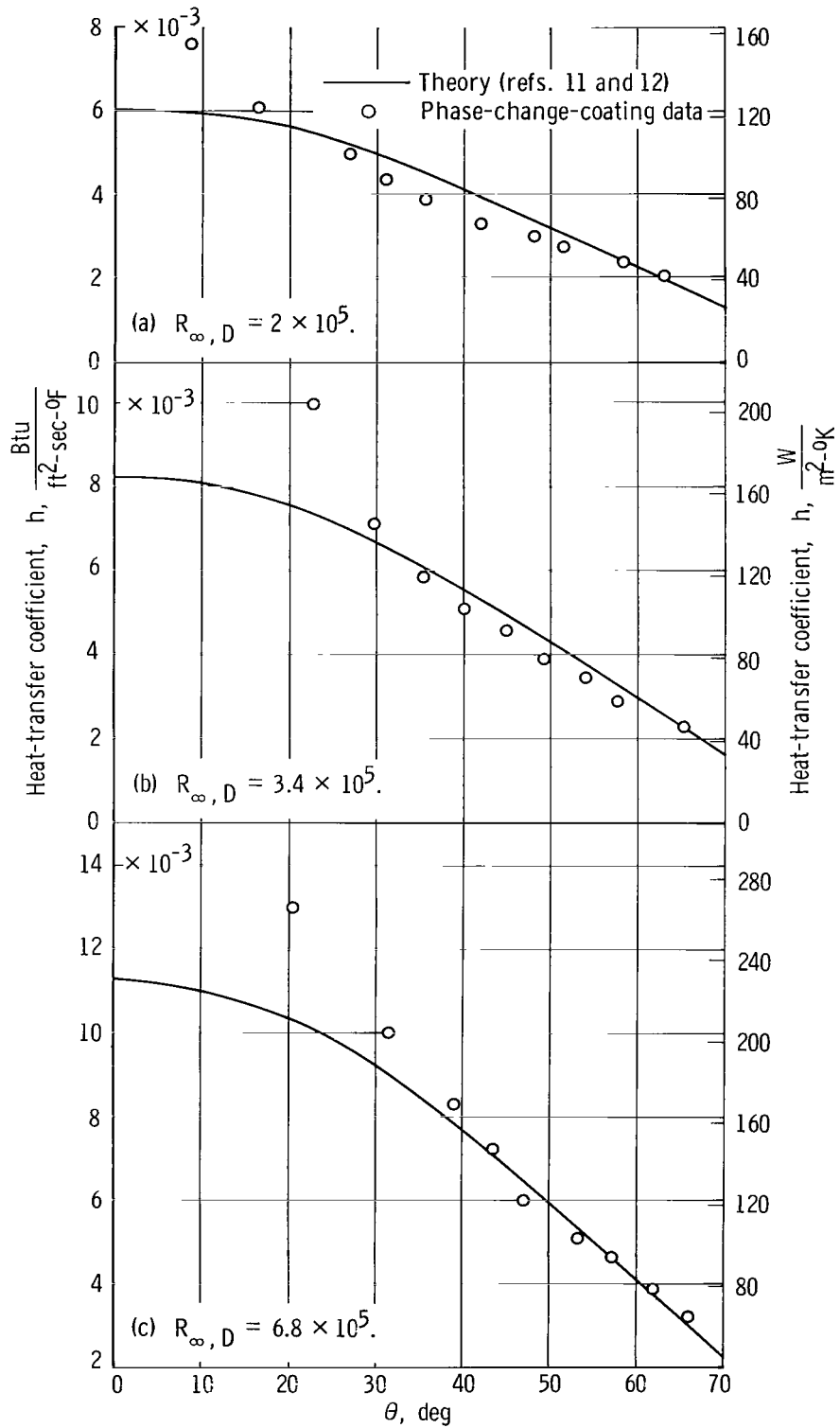


Figure 11.- Heat-transfer distribution on hemisphere-cylinder.

Several tests were made at each Reynolds number and the repeatability of the data was very good; therefore, only one set of data is shown. The theoretical heat-transfer coefficients were obtained by using a modified Newtonian pressure distribution with the method of reference 11 to determine the stagnation-point value and the method of reference 12 to determine the distribution. The experimental data are in relatively good agreement with the theoretical values except for the data point nearest the stagnation point for each of the three Reynolds numbers. These data points correspond to the earliest time for which data could be reduced - that is, considerably less than 1 second - and the error in h due to any error in determining the initial time is therefore large (figs. 8 and 9). These initial data are shown only to emphasize the point that the time required for the phase change to occur must be large compared with the time required to inject the model or large compared with the error in determining the initial time. For these tests the initial time was taken to be that of the first frame of film which showed the model to be in the tunnel free stream. Inasmuch as the model actually encountered the airflow a short time before this so-called initial time, the error in initial time is such as to always make the indicated heat-transfer coefficient larger than the actual value for very early times. The second data point shown in figures 11(a), (b), and (c) corresponds to a time less than 0.2 second after the first data point and is much closer to the theoretical values.

Segment of a Sphere at Angle of Attack

A comparison of heat-transfer data obtained by the phase-change-coating method with data obtained by the thermocouple-calorimeter method is presented in figure 12. The two sets of data were obtained on similar models at the same test conditions in the same facility. The phase-change model had a spherical radius r of 4.8 inches (12.19 cm) and a face diameter of 4 inches (10.16 cm) and was made from fiberglass-reinforced plastic. The thermocouple-calorimeter model was built to the same shape but was made from stainless steel with a 0.030-inch-thick (0.0762 cm) skin. Iron-constantan thermocouples were spot-welded to the inner surface of this thin skin. The data shown are for various locations along the vertical line of symmetry at an angle of attack of 35° . The small number of phase-change data points shown is due to the relatively low framing rate of the camera. Actually one could obtain as much data as desired by simply operating the camera at higher framing rates. Good agreement is indicated for these two methods of obtaining aerodynamic heat-transfer data.

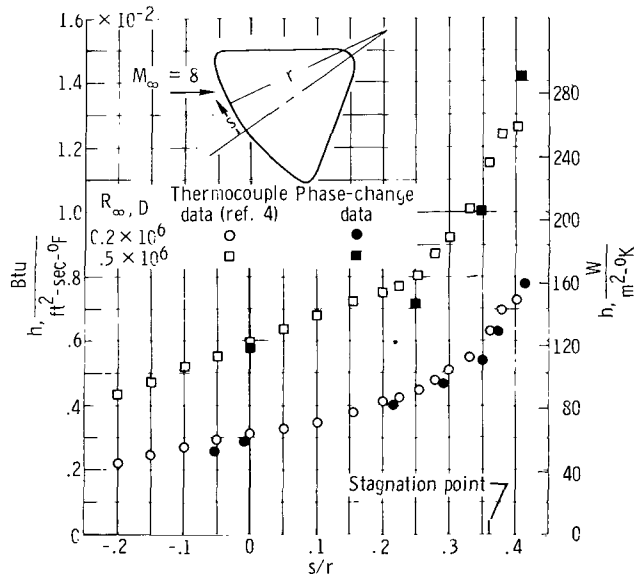


Figure 12.- Comparison of phase-change data with thermocouple-calorimeter data for a segment of a 4.8-inch-diameter sphere at an angle of attack of 35° .

Bell-Shaped Configurations

The heat-transfer coefficients on two bell-shaped configurations have been obtained with the phase-change method on models made from fiber-glass-reinforced plastic. From other tests of these configurations a rather extensive separated region was observed with reattachment somewhere on the flare as is indicated in the schlieren photographs of models 1 and 2 in figure 13. Consequently, these shapes would be expected to have areas in which the heat-transfer rates vary rapidly with surface distance and it might be difficult to detect the maximum or minimum rates with thermocouple-calorimeter techniques because of thermocouple spacing and lateral conduction. The phase-change-coating method however should provide a reasonably accurate measurement of these maximum and minimum rates. Sample photographs of the phase-change patterns obtained on model 2 are shown as figure 14. Notice the sharply defined region of very low heat-transfer rate just downstream of the nose. The measured heat-transfer coefficients for the two bell-shaped models are presented in figure 15; also included in the figure are sketches of the flow patterns. Large gradients in heating rate are indicated near the point of separation. For example, in figure 15(a) the heat-transfer coefficient varies by a factor of 4.5 over a surface distance of only 0.05 inch (0.127 cm). It is doubtful that heat-transfer rates could be accurately measured by the thermocouple-calorimeter technique in regions subjected to such large gradients. The present phase-change-coating method should therefore prove to be very useful for complex configurations. In reference 13 the phase-change-coating method was used to measure the heating rates in regions near holes, protuberances, and reaction-control jets on a 4-inch-diameter (10.16 cm) model of the Apollo command module. The detailed heat-transfer distributions obtained in the interference regions were very good, particularly so, considering the small model dimensions.

CONCLUDING REMARKS

A method whereby quantitative heat-transfer data on arbitrary shapes can be determined by using a phase-change coating has been developed. This coating is a fusible temperature indicator which undergoes a phase change from an opaque solid to a clear liquid at a known temperature. In this method the heat-transfer coefficients depend upon the time required for the phase change to occur as determined by motion-picture photography and the thermal properties of the model wall. Charts are presented of the aerodynamic heat-transfer coefficient as a function of the time required for the phase change to occur, the thermal properties of the model wall, and the temperature conditions of the test. Data obtained by this method and those obtained by use of aerodynamic theory and by the conventional thermocouple-calorimeter technique show close agreement. This agreement indicates that accurate data can be obtained with the phase-change-coating method.

Lateral conduction effects are minimized by the very low thermal conductivity and in effect the entire surface of a model is instrumented. Thus the present method appears particularly useful for complex configurations which are difficult to instrument with thermocouples or for configurations subjected to interference effects for which the desirable placement of thermocouples is not known beforehand. In addition, the models which are cast from plastic can be made quickly at low cost and the data are rapidly and easily reduced without complicated recording apparatus or electronic computers.

Langley Research Center,
National Aeronautics and Space Administration,
Langley Station, Hampton, Va., September 16, 1965.

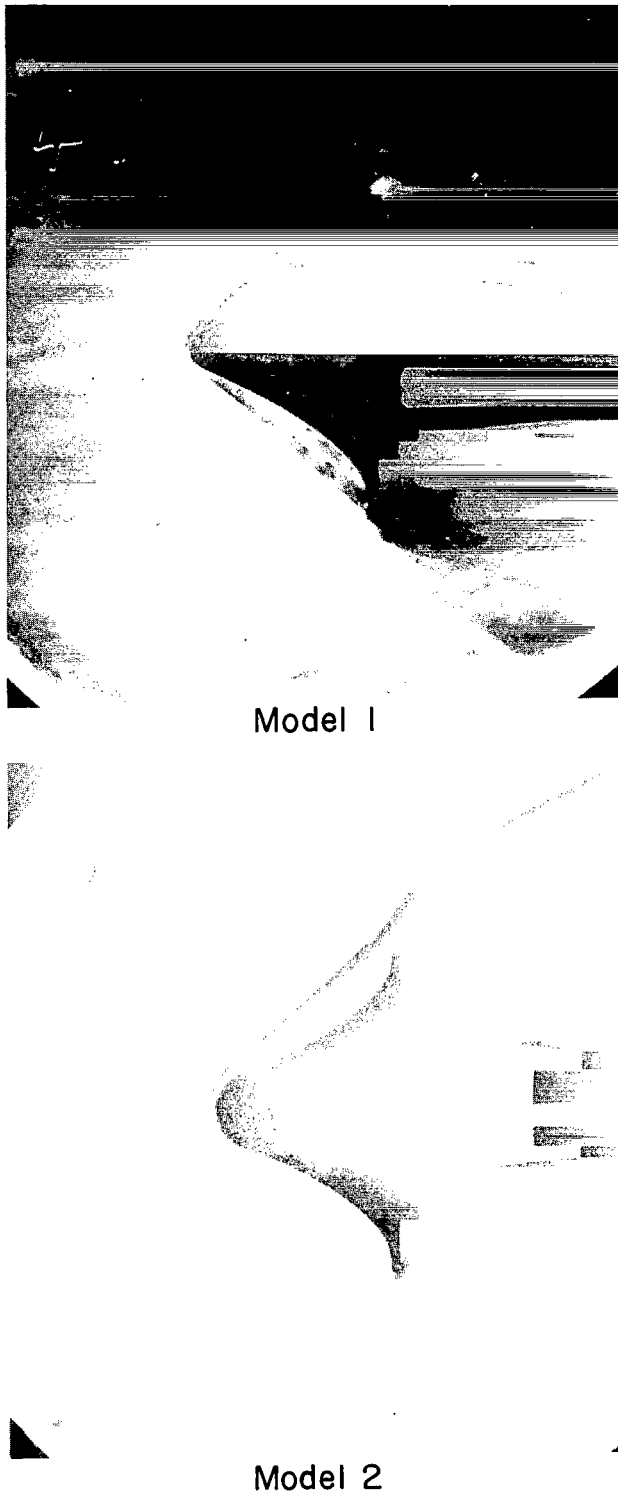
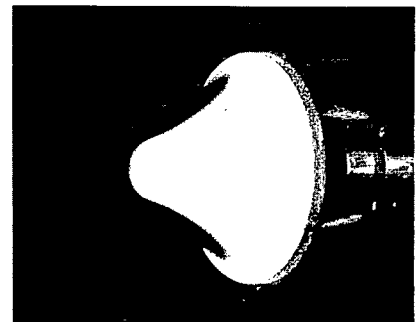


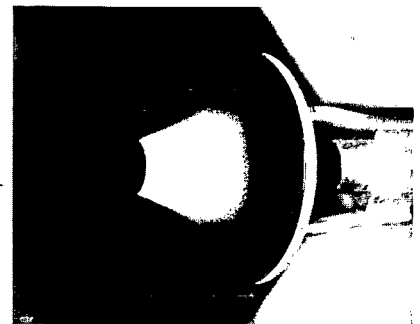
Figure 13.- Schlieren photographs of bell-shaped models at $R_{\infty,D} = 8 \times 10^5$. L-65-7967

No flow

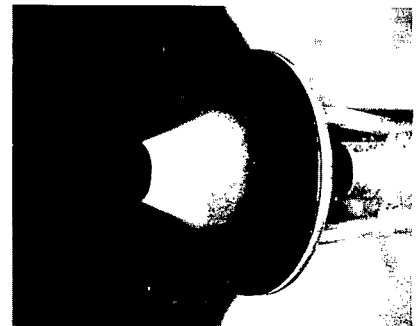


$T_{pc} = 200^\circ \text{ F}$
(366.5° K)

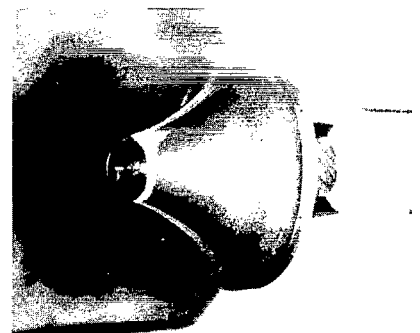
Flow →



$t = 0.3 \text{ sec}$



$t = 1.1 \text{ sec}$



$t = 3.75 \text{ sec}$

Figure 14.- Phase-change patterns on bell-shaped model 2. $T_{DC} = 200^\circ \text{ F}$. L-65-7968

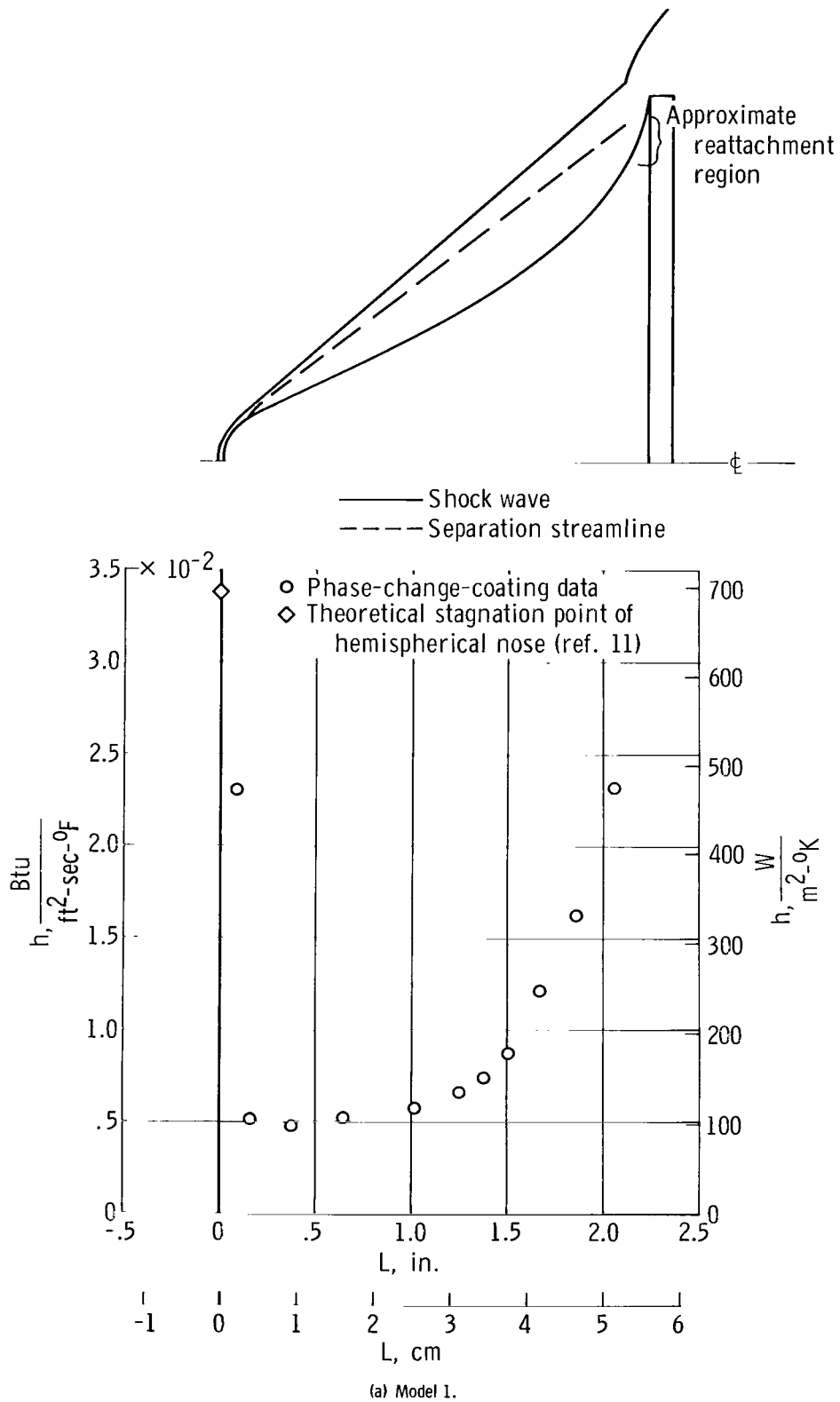
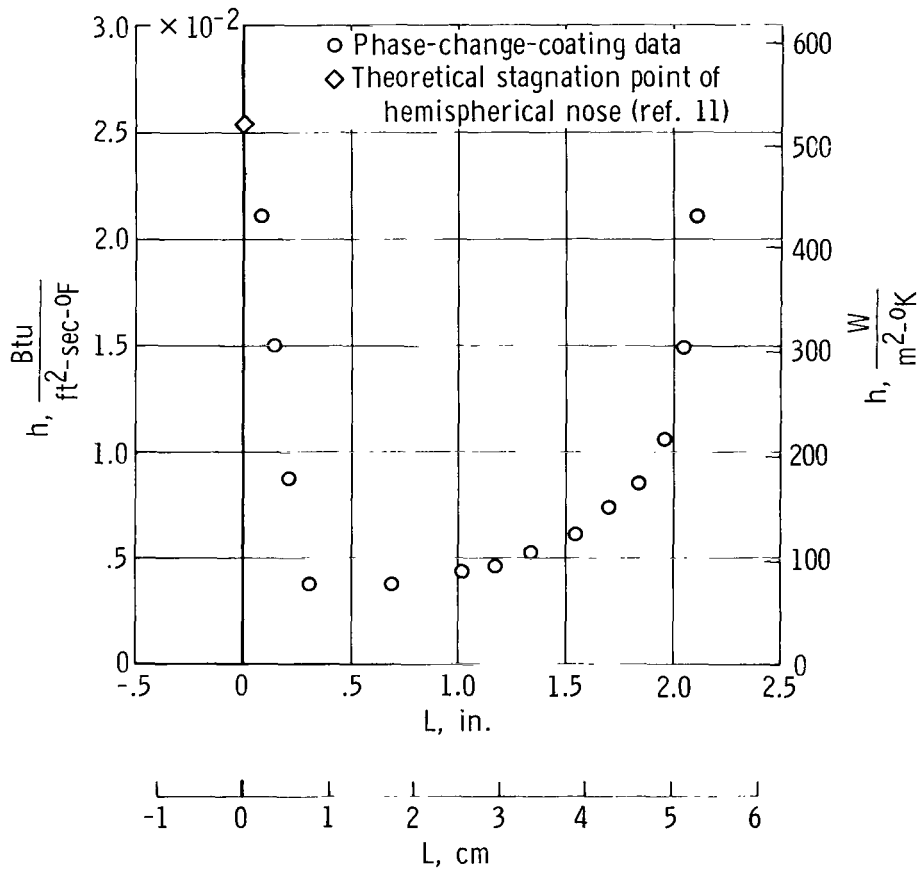
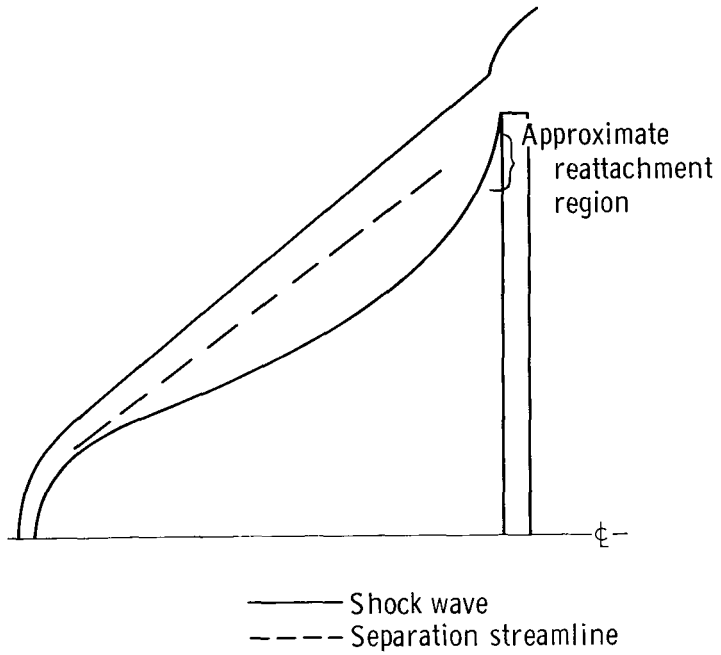


Figure 15.- Heat-transfer distribution on bell-shaped models (base diameter = 4 inches). $R_{\infty, D} = 8 \times 10^5$.



(b) Model 2.

Figure 15.- Concluded.

APPENDIX A

ERRORS INDUCED BY THE PRESSURE DEPENDENCE
OF COLOR-CHANGE COATINGS

The dependence of the color-change temperature on ambient pressure could introduce an error into the reference body method unless the pressures on the reference body and the model were equal at each location where a simultaneous color change occurred. In addition, a pressure-dependent color change would increase the complexity of a theoretical solution to such an extent as to render it impractical. With this in mind, several color-change coatings were calibrated for pressure effects by using the technique described in the section "Phase-Change Coatings." Some coatings were much more sensitive to ambient pressure than others; however, all coatings tested were affected by pressure to some extent. Figure 16 shows the pressure dependence of the pink-to-blue color change of one of the four color-change coatings which has been used extensively in wind-tunnel tests. The plot shows the temperature at which the pink-to-blue color change occurred as a function of the heating time for ambient pressures of 3 and 760 mm of mercury absolute (400 and 101 325 N/m²). A considerable pressure dependence is indicated in these data.

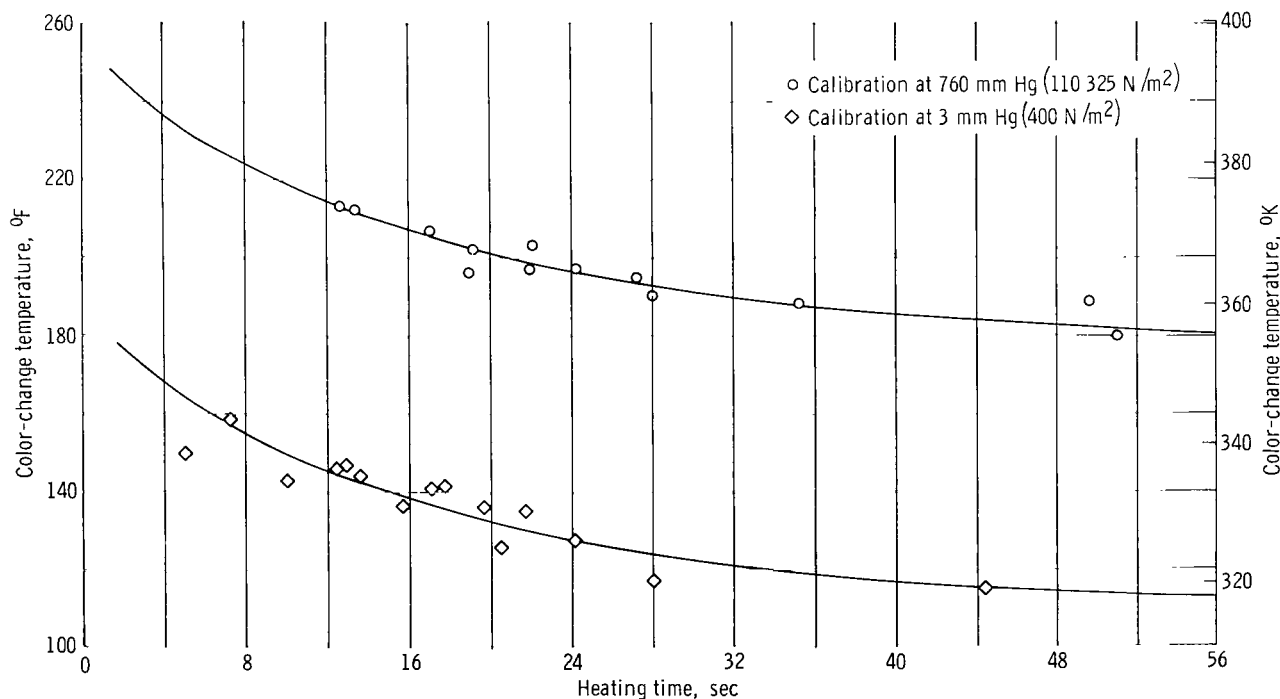


Figure 16.- Variation of color-change temperature with heating time for pink-to-blue color change.

APPENDIX A

Figure 17 is a plot of the same data with the color-change temperature as a function of the temperature rise rate of the coating. Curves of the form

$$T_{cc} = A + B \frac{dT}{dt} + C \left(\frac{dT}{dt} \right)^2 \quad (A1)$$

are shown as solid lines in this figure. To obtain an indication of the error that could be induced by neglecting this pressure effect, equation (A1) for the color-change temperature (assumed valid for $t > 2$ sec) and equation (5) for the model surface temperature

$$\frac{T - T_i}{T_{aw} - T_i} = 1 - e^{-\beta^2} \operatorname{erfc} \beta$$

were solved simultaneously to give

$$\begin{aligned} \frac{T_{cc} - T_i}{T_{aw} - T_i} = & 1 - e^{-\beta^2} \operatorname{erfc} \beta - B \left(\frac{\beta}{t} \right) \left(\frac{1}{\sqrt{\pi}} - \beta e^{-\beta^2} \operatorname{erfc} \beta \right) \\ & - C (T_{aw} - T_i) \left(\frac{\beta}{t} \right)^2 \left(\frac{1}{\sqrt{\pi}} - \beta e^{-\beta^2} \operatorname{erfc} \beta \right)^2 \end{aligned} \quad (A2)$$

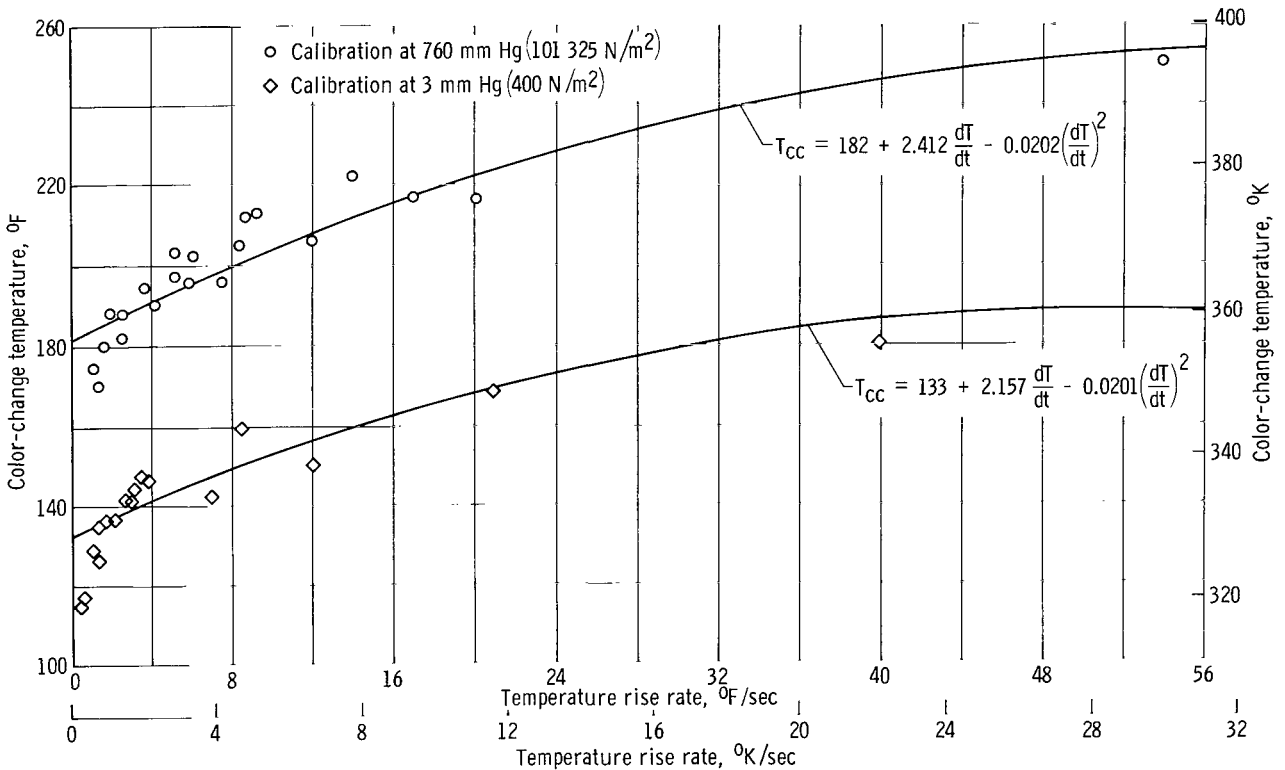


Figure 17.- Variation of color-change temperature with temperature rise rate for pink-to-blue color change. (T_{cc} and T are in $^{\circ}\text{F}$. See figure 18 for equivalent SI values for terms of equations.)

APPENDIX A

A working form of the solution of equation (A2) is given in figure 18 for the two calibrations in figure 17 in terms of $\frac{h}{k}\sqrt{\alpha}$ as a function of time for an initial temperature T_i of 80° F (299.8° K) and an adiabatic wall temperature T_{aw} of 1100° F (866.5° K). If the thermal properties of the model k and $\sqrt{\alpha}$ are assumed to be constant, the indicated heat-transfer coefficient for the 3 mm of mercury calibration curve is about one-half that obtained with the 760 mm of mercury calibration curve for all test times from 2 to 25 seconds. Therefore, if the reference model method were used under conditions for which the pressures on the test model and the reference model were 3 and 760 mm of mercury (400 and $101\,325\text{ N/m}^2$), respectively, at locations where color changes occurred at equal times, the indicated heat-transfer coefficient would be in error by a factor of 2.

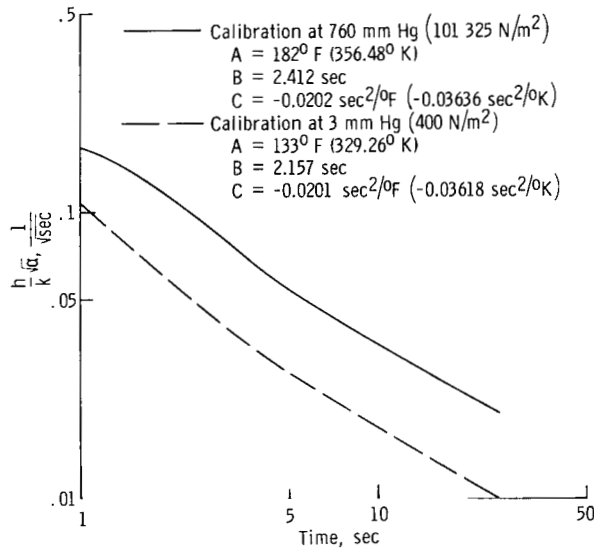


Figure 18.- Solution of equation (A2). $T_{aw} = 1100^\circ\text{ F}$ (866.5° K);
 $T_i = 80^\circ\text{ F}$ (299.8° K).

APPENDIX B

CONVERSION OF U.S. CUSTOMARY UNITS TO SI UNITS

The International System of Units (SI) was adopted by the Eleventh General Conference on Weights and Measures held in Paris, October 1960, in Resolution No. 12 (ref. 6). Conversion factors required for units used herein are given in the following table:

Physical quantity	U.S. Customary Unit	Conversion factor (*)	SI Unit
Density	lb/ft ³	16.0185	kilograms/meter ³ (kg/m ³)
Heat-transfer coefficient . .	Btu/ft ² -sec-°F	2.0428 × 10 ⁴	watts/meter ² -degrees Kelvin (W/m ² -°K)
Length	{ in.	2.54 × 10 ⁻²	meters (m)
	{ ft	3.048 × 10 ⁻¹	meters (m)
Pressure	mm Hg	1.333 × 10 ²	newtons/meter ² (N/m ²)
Specific heat . .	Btu/lb-°F	4.184 × 10 ³	joules/kilogram-degrees Kelvin (J/kg-°K)
Temperature . . .	(°F + 459.67)	5/9	degrees Kelvin (°K)
Temperature rise rate . . .	°F/sec	5/9	degrees Kelvin/second (°K/sec)
Thermal conductivity . .	Btu/ft-sec-°F	6.2265 × 10 ³	joules/meter-second-degrees Kelvin (J/m-sec-°K)
Thermal diffusivity . .	ft ² /sec	9.2903 × 10 ⁻²	meters ² /second (m ² /sec)

*Multiply value given in U.S. Customary Unit by conversion factor to obtain equivalent value in SI Unit.

Prefixes to indicate multiples of units are as follows:

Prefix	Multiple
kilo (k)	10 ³
centi (c)	10 ⁻²

REFERENCES

1. Stainback, P. Calvin: A Visual Technique for Determining Qualitative Aerodynamic Heat Rates on Complex Configurations. NASA TN D-385, 1960.
2. Anon.: Calibration Curves for Temperature Indicating Colors, Detectotemp and Thermochrom. Rept. No. R-4a, Princeton Div., Curtiss-Wright Corp., July 1959.
3. Lorenz, George C.; Sartell, Robert J.; and Strack, Sainsbury L.: Experimental Investigation of Heat Transfer to Complex Aerodynamic Configurations at Hypersonic Speeds. ASD-TDR-63-530, U.S. Air Force, Sept. 1963.
4. Jones, Robert A.; and Hunt, James L.: Use of Temperature-Sensitive Coatings for Obtaining Quantitative Aerodynamic Heat-Transfer Data. AIAA J., vol. 2, no. 7, July 1964, pp. 1354-1356.
5. Kasanoff, D. R.; and Kimmel, E.: Recent Developments in Fusible Temperature Indicators. Temperature - Its Measurement and Control in Science and Industry, vol. 3, pt. 2, Reinhold Pub. Corp., c.1962, pp. 1005-1007.
6. Mechtly, E. A.: The International System of Units - Physical Constants and Conversion Factors. NASA SP-7012, 1964.
7. Carslaw, H. S.; and Jaeger, J. C.: Conduction of Heat in Solids. Second ed., Oxford Univ. Press, Inc., 1959, p. 71.
8. Swann, Robert T.; and Pittman, Claud M.: Numerical Analysis of the Transient Response of Advanced Thermal Protection Systems for Atmospheric Entry. NASA TN D-1370, 1962.
9. Traiger, Harris L.; and Wentworth, Ralph L.: Thermophysical Properties Measurements Performed for NASA. Rept. No. 493, Dynatech Corp., Aug. 27, 1964.
10. Stainback, P. Calvin: Heat-Transfer Measurements at a Mach Number of 8 in the Vicinity of a 90° Interior Corner Alined With the Free-Stream Velocity. NASA TN D-2417, 1964.
11. Reshotko, Eli; and Cohen, Clarence B.: Heat Transfer at the Forward Stagnation Point of Blunt Bodies. NACA TN 3513, 1955.
12. Lees, Lester: Laminar Heat Transfer Over Blunt-Nosed Bodies at Hypersonic Flight Speeds. Jet Propulsion, vol. 26, no. 4, Apr. 1956, pp. 259-269, 274.
13. Jones, Robert A.; and Hunt, James L.: Effects of Cavities, Protuberances, and Reaction-Control Jets on Heat Transfer to the Apollo Command Module. NASA TM X-1063, 1965.

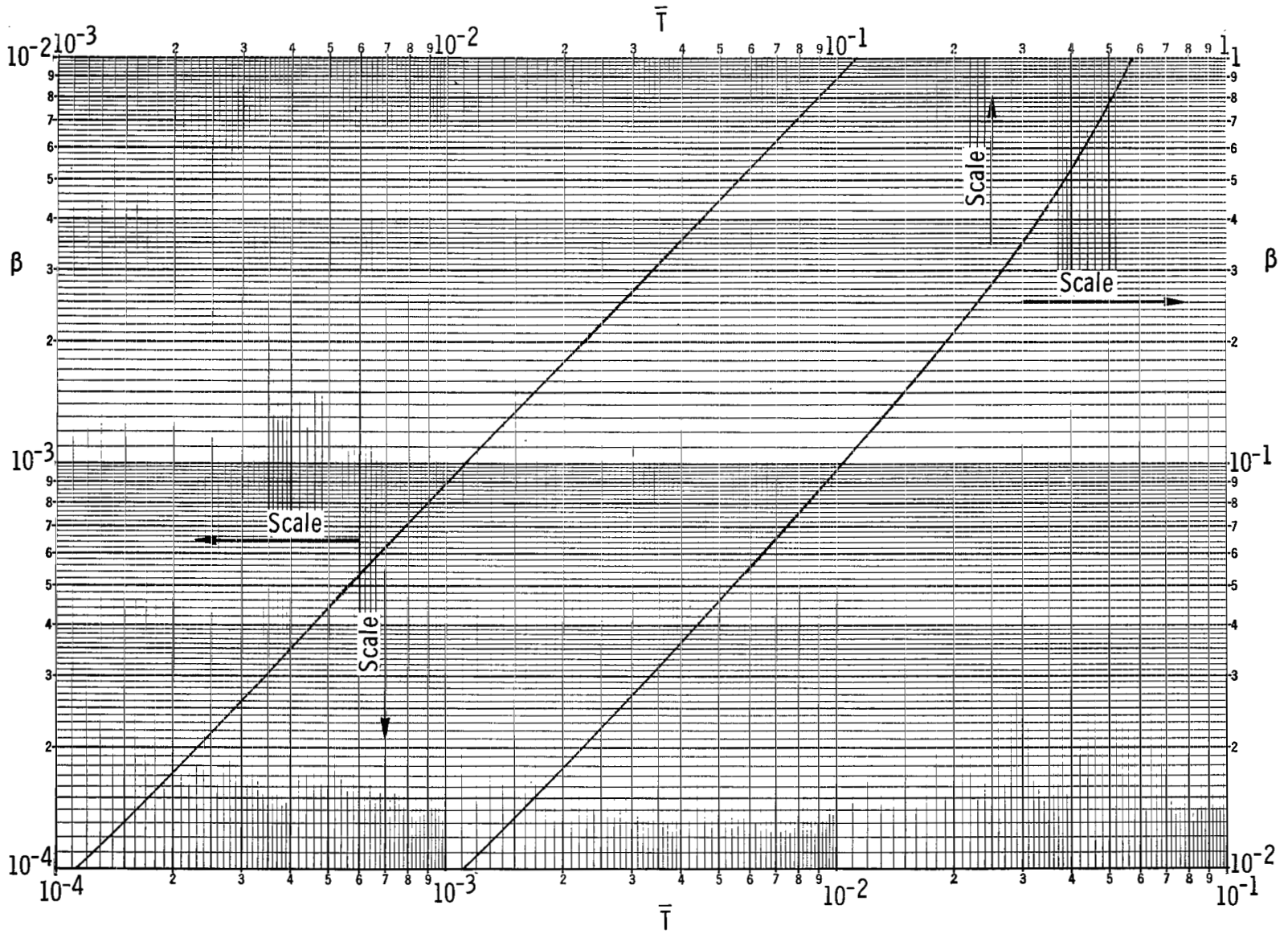


Figure 4.- Solution of heat-conduction equations (plot of eq. (5)).

"The aeronautical and space activities of the United States shall be conducted so as to contribute . . . to the expansion of human knowledge of phenomena in the atmosphere and space. The Administration shall provide for the widest practicable and appropriate dissemination of information concerning its activities and the results thereof."

—NATIONAL AERONAUTICS AND SPACE ACT OF 1958

NASA SCIENTIFIC AND TECHNICAL PUBLICATIONS

TECHNICAL REPORTS: Scientific and technical information considered important, complete, and a lasting contribution to existing knowledge.

TECHNICAL NOTES: Information less broad in scope but nevertheless of importance as a contribution to existing knowledge.

TECHNICAL MEMORANDUMS: Information receiving limited distribution because of preliminary data, security classification, or other reasons.

CONTRACTOR REPORTS: Technical information generated in connection with a NASA contract or grant and released under NASA auspices.

TECHNICAL TRANSLATIONS: Information published in a foreign language considered to merit NASA distribution in English.

TECHNICAL REPRINTS: Information derived from NASA activities and initially published in the form of journal articles.

SPECIAL PUBLICATIONS: Information derived from or of value to NASA activities but not necessarily reporting the results of individual NASA-programmed scientific efforts. Publications include conference proceedings, monographs, data compilations, handbooks, sourcebooks, and special bibliographies.

Details on the availability of these publications may be obtained from:

SCIENTIFIC AND TECHNICAL INFORMATION DIVISION
NATIONAL AERONAUTICS AND SPACE ADMINISTRATION

Washington, D.C. 20546